THE JOURNAL OF PHYSICAL CHEMISTRY C

ARTICLE

pubs.acs.org/JPCC

Highly Ordered Carbon Nanotube Nematic Liquid Crystals

Nicolas Puech,[†] Christophe Blanc,[‡] Eric Grelet,[†] Camilo Zamora-Ledezma,[§] Maryse Maugey,[†] Cécile Zakri,[†] Eric Anglaret,[‡] and Philippe Poulin[†,*]

[†]Centre de Recherche Paul-Pascal, Université de Bordeaux — CNRS, 115 Avenue Schweitzer, 33600 Pessac, France

[‡]Université Montpellier 2 et CNRS, Laboratoire Charles Coulomb UMR 5221, place Eugène Bataillon, F-34095, Montpellier, France

[§]Laboratorio de Física de la Materia Condensada, Centro de Física, Instituto Venezolano de Investigaciones Científicas, Altos de Pipe, 1024 Caracas, Venezuela

ABSTRACT: Liquid crystal ordering is an opportunity to develop novel materials and applications with carbon nanotubes spontaneously aligned on macroscopic scales. Nevertheless, achievement of large orientational order parameter and extended monodomains remains challenging. In this work, we show that shortening nanotubes allows the formation of liquid crystals that can easily be oriented under the form of large macroscopic monodomains. The orientational order parameter of single-wall nanotube liquid crystals measured by polarized Raman spectroscopy at the isotropic—nematic transition exceeds by far the value reported in previous experiments. The presently measured order parameter approaches the value theoretically expected for liquid crystals made of rigid rods in solution. This finding suggests that the production of highly ordered nanotube-based liquid crystals was presumably limited in earlier contributions by the length and waviness of long nanotubes. Both factors increase the material viscosity, can yield some elasticity, and stabilize topological defects.

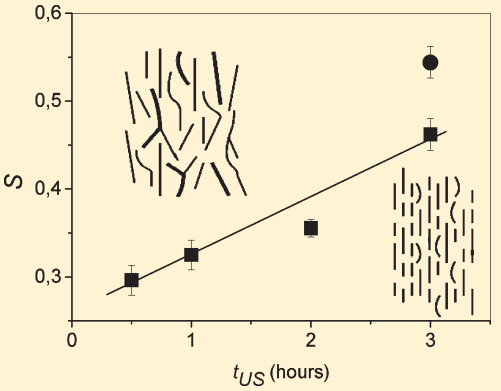

INTRODUCTION

Carbon nanotubes can be produced on a large scale by several techniques: arc discharge, chemical vapor deposition, or laser ablation.[1] All of these methods generally lead to powderlike soots made of disordered single-wall nanotubes or multiwall nanotubes. Various approaches have been explored over recent years to process nanotubes into oriented materials and achieve enhanced properties: application of external fields,[2−5] fiber spinning and drawing,[6−11] dispersion in organized solvents,[12−19] and so forth. Forming liquid crystals is one of the most appealing approaches. Indeed liquid crystal transition is a thermodynamic phenomenon that spontaneously takes place when the nanotubes are homogeneously suspended in a liquid medium at a sufficiently high concentration. Phases of orientationally ordered particles are called nematic liquid crystals. This type of self-organized structure has been observed with carbon nanotubes[20−33] and a number of other anisotropic particles such as inorganic rods,[34,35] cellulose whiskers,[36] viruses,[37,38] and so forth. Above a certain concentration, the entropy becomes maximized with the long-range orientation of the nanotubes. The loss of orientational entropy is compensated by the minimization of the excluded volume of the oriented particles and the associated increase of packing entropy.[39] These systems are thermodynamically stable and their degree of ordering is usually quantified by a scalar called the orientational order parameter S. $S = \langle 3\cos^2\theta - 1\rangle/2$, where θ is the angle between a particle axis and the director that is the vector that specifies the average alignment direction of the particles ($S = 0$ for an isotropic system and $S = 1$ for a perfect alignment). According to Onsager's predictions[39] for hard and rigid rods, S is expected to be of 0.79 at the isotropic—nematic transition. Such high values of the order parameter have been actually measured in several liquid crystals made of rodlike particles.[40,41] However, the situation remains challenging for carbon nanotube liquid crystals. These materials often exhibit a high density of topological defects.[28,31] Nanotubes stabilized in water by single-stranded DNA molecules can exhibit nematic ordering with a phase diagram consistent with the Onsager's prediction.[23] Such liquid crystals could be oriented over large monodomains through shear induced alignment procedures; offering thereby the opportunity to measure the nematic order parameter S.[28] However, in spite of phase boundaries consistent with Onsager's predictions, the values of the order parameter S measured by micro-Raman polarized spectroscopy on aligned and dried films was much smaller than expected.[28] This paradox raises questions about the origin of such a low value. The measurement method was successfully validated with the same diluted nanotubes embedded in a stretched polymer.[42] Lu and Chen[27] recently demonstrated that impurities could greatly hinder the ordering of nanotubes in concentrated suspensions and showed that purified nanotubes could be efficiently shear-aligned in composite membranes. Nevertheless, nanotubes of relatively high purity were also used in other studies[28,31] and could not lead

Received: October 25, 2010
Revised: December 14, 2010
Published: February 04, 2011

   dx.doi.org/10.1021/jp1102077 | *J. Phys. Chem. C* 2011, 115, 3272–3278

to materials aligned on macroscopic scale. Song and Windle[31] have shown that the morphology of the nanotubes can affect the texture of nematic liquid crystals and the density of topological defects. In particular, the authors have demonstrated that long nanotubes could be bent around the core of topological defects. The stabilization of topological defects by deformed or imperfect nanotubes could explain the difficulty in aligning such materials over large monodomains. Even shear aligned and dried materials could indeed still contain defects at the microscopic scale, which can neither be visualized by optical microscopy nor detected by polarized Raman spectroscopy. Such techniques, as other optical or scattering techniques, probe a surface area of a few micrometers square. Topological defects could be stabilized by long and deformed nanotubes and yield apparent low-order parameters. Long and/or tortuous nanotubes can also increase the viscosity of the material and even yield some elastic behavior that hinders the spontaneous coarsening of topological defects as observed in conventional liquid crystals.[43,44] Quantitative clarifications of these questions are critical to achieve carbon nanotube liquid crystals with a greater degree of ordering. In this work, we investigate the behavior of carbon nanotubes that have been shortened by sonication[45,46] and stabilized by bile salt molecules. Bile salts have been already shown to be excellent dispersants for carbon nanotubes.[47] The shorter nanotubes are in addition sorted by centrifugation experiments.[48] Liquid crystals have been made by dispersing these sorted nanotubes in water. We find that short nanotubes can easily be aligned over large monodomains by shear induced treatments. More importantly, it is observed that dry films made from aligned monophasic liquid crystals exhibit orientational order parameters up to $S = 0.55$. As already reported in a previous study of related materials,[28] the order parameter of the sample does not evolve during drying. In principle, concentration increase should yield an increase of the order parameter during water evaporation. Nevertheless, the increase of nanotube concentration is also associated to an increase of viscosity and slowing down of the sample dynamics. These effects prevent structural changes during the fast evaporation of the solvent and can explain the quenching of the order parameter. In addition, we also report the observation of uniform tactoids at the isotropic−nematic equilibrium. The presence of tactoids reflects the remarkable alignment of the nanotubes into fluid droplets. The observation of such tactoids is a unique opportunity to probe a nematic monodomain and measure more accurately the order parameter of a nanotube-based liquid crystal. To our knowledge, this is the first measurement of the order parameter of a nondried nanotube liquid crystal. Such measurements are made possible in the present case because the size of the observed tactoids is greater than the size of the laser beam used in the Raman experiments. The order parameter is found to be of 0.65. This first quantitative characterization is in relatively good agreement with the theoretically expected behavior of rigid rods in solution.

MATERIALS AND METHODS

The starting CNT material is a wet cake-like material made of purified and highly hydrated CNTs. The wet cake contains 15 wt % of carbon nanotubes. It was provided by Thomas Swan (UK) under the trade name Elicarb (batch number K3778, http://www.thomas-swan.co.uk). The CNTs are assembled in the wet cake as bundles and entangled aggregates. Even though such nanotubes are provided as single-wall materials, they contain a small fraction of double- and triple-wall nanotubes. These CNTs were suspended in aqueous solutions of bile salts. The bile salts used in this work were purchased from Fluka. They are made of a mixture of cholate sodium salt and deoxycholate sodium salt (respectively 50% and 50% w/w). Bile salts (BS) are short amphiphilic and asymmetric molecules that have been already shown to be efficient at stabilizing nanotubes in water.[47] A commercial mixture is used in the present experiments. Nevertheless, it was shown that cholate sodium salt or deoxycholate sodium salt can also be used individually as effective nanotube dispersants.[50] The dispersions were homogenized by sonication. All of the sonication experiments were performed in 10 cm^3 aqueous solutions, which contain 0.5 wt % CNTs and 0.5 wt % of BS. It is possible that varying the relative fraction of BS and CNT could affect the interactions between the CNT and the phase behavior of the systems. But this factor was kept constant for all of the presently investigated samples. Sonication was performed using a Branson Sonifier S-250A equipped with a 13 mm step disruptor horn and a 3 mm tapered microtip, operating at a 20 kHz frequency. The homogeneity of the dispersions at the micrometer scale has been checked by optical microscopy. BS dispersants allow an effective debundling of the nanotubes. The repulsive interactions they provide prevent the nanotubes from reforming bundles. As indicated further, debundling of the CNTs is confirmed by the observation of photoluminescence. Starting with low concentrations allows homogeneous dispersions to be easily achieved. However, the systems do not form liquid crystals at such concentrations. The samples have to be ultracentrifuged to achieve greater concentrations.[28] Fagan et al. recently investigated the sedimentation of carbon nanotubes and concluded that longer nanotubes sediment faster than short nanotubes under ultracentrifugation;[48] offering thereby the opportunity to sort nanotubes by their length. After the sonication treatments, the biggest aggregates and large bundles are removed via a gentle centrifugation: 2700 g for 30 min. The supernatant is collected and ultracentrifuged at 210 000 g for various durations from 30 min to 3 h at room temperature ($T = 20$ °C). Ultracentrifugation allows the concentration of the nanotubes at the bottom of the vial to be increased. When the concentration is sufficiently large, the systems are expected to form a nematic phase at the bottom of the vial. The concentrated sediments (nanotube fraction typically above 5 wt % as measured by thermogravimetric analyses) are separated from the remaining supernatants and homogenized by vigorous mixing. An optical micrograph of such concentrated sediment in the transmission mode between crossed polarizers is shown in part a of Figure 1. The variations of transmitted light intensity are due to the strong dichroism of oriented CNTs. They reflect the liquid crystallinity of the material. This concentrated system forms indeed a monophasic nematic liquid crystal. However, the inhomogeneous texture shown in part a of Figure 1 reveals the absence of spontaneous alignment and of large monodomains. Macroscopic alignment can be achieved via shear induced alignment. A droplet of liquid crystal is sandwiched between two glass slides and sheared by moving the upper slide as already shown in ref 28. The upper slide is removed to allow the quick drying of the thin film upon water evaporation. Such dried films can be more easily studied because the slides do not have to be sealed right after the shear to keep the concentrations and chemical potential constants. But as already reported in a previous study of related materials,[28] the order parameter of the sample does not evolve during drying. It is believed that this absence of evolution is arising from the high viscosity of the

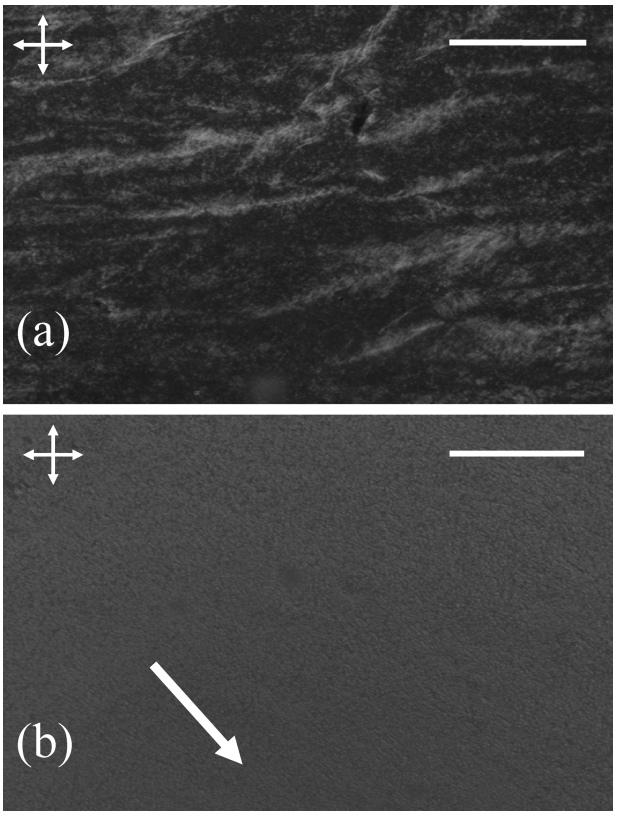

Figure 1. Optical micrographs between crossed polarizers in transmission mode of (a) a CNT liquid crystal between a glass slide and a coverslip and of (b) a dried film of the same material that has been homogeneously shear-orientated. The shear axis is specified by the white arrow. The directions of the crossed polarizers are specified by the crossed arrows in the upper-left corners of the pictures. Scale bar, 200 μm.

materials and from the fast rate of drying. The time taken for drying is too short to allow substantial structural changes. An optical micrograph of a dry film is shown in part b of Figure 1. The intensity is homogeneous across the sample; indicating an apparent uniform orientation of the CNTs at the resolution of the optical microscopy. Deeper studies of such films have been performed using polarized Raman spectroscopy. In particular, the orientational order parameter was measured as a function of the sonication and centrifugation treatments of the CNT dispersions. The increase of the CNT concentration during drying could be expected to yield an increase of the order parameter. Nevertheless, as indicated above, it was shown that the order parameter of such materials does not evolve during drying.[28] Characterizations in the liquid state have been performed with dilute systems. Concentrated samples can indeed be diluted in order to reach the diphasic isotropic−nematic domain. Nematic tactoids are observed at the isotropic−nematic equilibrium. From a technical point of view, the glass slides can here be easily sealed with epoxy glue before characterizations without perturbing the system because the continuous phase is isotropic.

RESULTS AND DISCUSSION

It is known that sonication induces the scission of carbon nanotubes. The nanotube length decreases with sonication time and power.[45,46] We first qualitatively checked the influence of sonication and ultracentrifugation time on the length of the nanotubes. We quantitatively investigated in a second step their effect on the order of nanotube-based nematic liquid crystals. We investigated materials at, or close to, the isotropic−nematic transition to achieve comparisons of order parameters in similar thermodynamical conditions. Whereas the phase boundaries have not been determined accurately for all the samples, it was observed that the systems were in monophasic isotropic states for nanotube weight fractions typically below 3 wt % and in monophasic nematic states for nanotube weight fractions typically above 5 wt %. Isotropic−nematic equilibrium was achieved in between those boundaries. TEM was used to confirm the expected effect of sonication and ultracentrifugation for two different BS-stabilized CNT suspensions. The suspensions have been prepared at two different sonication t_{US} and ultracentrifugation times $t_{UC:}$

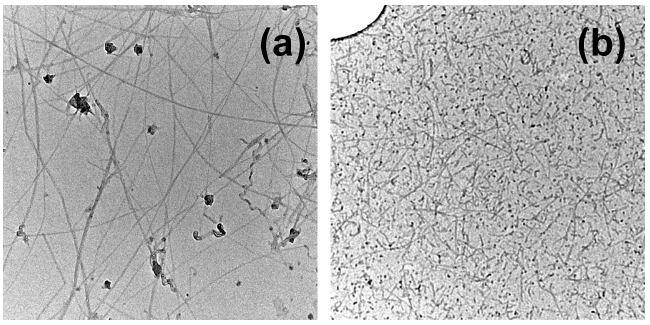

Figure 2. Transmission electron microscopy of CNTs after (a) 30 min of sonication and 45 min of ultracentrifugation, (b) 3 h of sonication and 3 hours of ultracentrifugation. Scale: the images' size is 1.5 × 1.5 μm.

Sample A: 30 min sonication and 45 min ultracentrifugation at 210 000 g

Sample B: 3 h sonication and 3 h ultracentrifugation at 210 000 g

Centrifugates were collected after ultracentrifugation. Their concentration was determined via thermogravimetric analyses. Then these materials were diluted in water at a weight fraction of about 10^{-4} wt%. The TEM pictures in Figure 2 show the strong impact of sonication and ultracentrifugation on the length and morphology of the nanotubes. It is difficult to provide a reliable statistical analysis of TEM images because only a few nanotubes can be observed on each picture. Nevertheless, even if still qualitative, the present TEM images demonstrate that the length and the diameter of CNT clearly decrease for long sonication and ultracentrifugation times. Branched nanotubes and kinks of long nanotubes can be seen in weakly sonicated materials. By contrast shorter nanotubes appear to be straighter.

More samples have been prepared in different conditions to make dried films and characterize their order parameter. The laser excitation is a polarized Nd:YAG laser operating at 1064 nm and a polarization analyzer was used to determine the average alignment of the CNTs. Figure 3 shows the typical Raman spectra of orientated CNTs films obtained after shear-induced alignment of CNT liquid crystals.[28] The spectra display the typical RBM, D, G, and G′ bands of CNTs and are consistent with the presence of a mixture of single-wall and double-wall nanotubes.[49] As already reported, photoluminescence is observed in dispersions and liquid films.[28] This observation indicates that a large fraction of CNTs are either individualized or assembled into

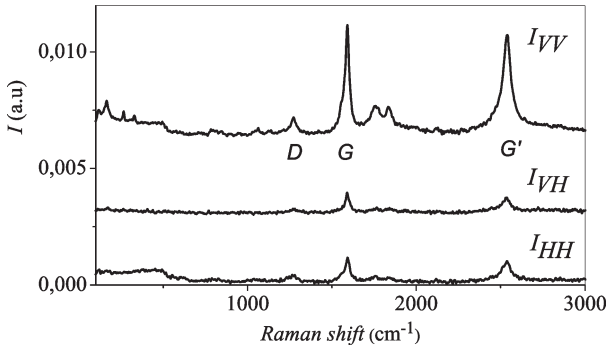

Figure 3. Polarized Raman spectra of a dry film in the three polarization configurations: I_{VV}, I_{VH}, and I_{HH}. The signal is strongly polarized and exhibits a maximal value for the *VV* configuration. This is clearly seen for the *D*, *G*, and *G*′ Raman bands.

bundles of only a few nanotubes even after a short sonication time of 30 min. Photoluminescence of the CNT dispersions does not evolve with time and confirms thereby the good stability of the samples. The Raman spectra of an oriented domain shown in Figure 3 are obtained in the three main polarization configurations, I_{VV}, I_{HH}, and I_{VH} where the first and second subscripts respectively refer to the polarizations of incident and scattered beams, oriented either parallel *V* or perpendicular *H* to the shear direction. The scattered intensity in the *VV* configuration is much greater than the intensity for the two other ones, showing the good alignment of nanotubes along the shear direction.

The orientational order parameter is computed from the intensity peak of the G-band fitted by two Lorentzian peaks. For a dilute suspension *S* is given by:[28]

$$S = \frac{3I_{VV} + 3I_{VH} - 4I_{HH}}{3I_{VV} + 12I_{VH} + 8I_{HH}} \qquad \text{(eq.1)}$$

This expression was introduced and validated experimentally for single-wall CNTs[28,42] but it is reasonable to use it also for double-wall CNTs and a fortiori for a sample containing both types of nanotubes. Nevertheless, the optical absorption of CNTs in opaque films cannot be neglected. The absorption depends on the CNT orientation, being maximal in the nanotube direction. It therefore attenuates the I_{VV} signal. Dichroism can be taken into account through the corrected expression:

$$S = \frac{6\Delta I_{VV} + 3(1+\Delta)I_{VH} - 8I_{HH}}{6\Delta I_{VV} + 12(1+\Delta)I_{VH} + 16I_{HH}} \qquad \text{(eq.2)}$$

where the dichroic ratio Δ is the ratio of absorbances at 1064 nm respectively along the *V* and *H* directions. The value of the order parameter *S* as a function of the nanotube sonication time t_{US} is reported in part a of Figure 4. Films made from liquid crystals of long CNTs exhibit a small order parameter ($S = \sim 0.3$). This can be understood by the presence of defects and kinks on the surface of the longest CNTs or even permanent junctions of nanotubes at the origin of an orientational disorder. This is schematically sketched in the left insert of part a of Figure 4. In contrast, the right insert shows improved alignment brought by shortening and sorting nanotubes by ultracentrifugation. The high viscosity of samples containing long CNTs can also explain the difficulty in aligning the materials. Considering these possible limitations, the order parameter is expected to be improved by selecting shortened and individualized nanotubes such as those produced after

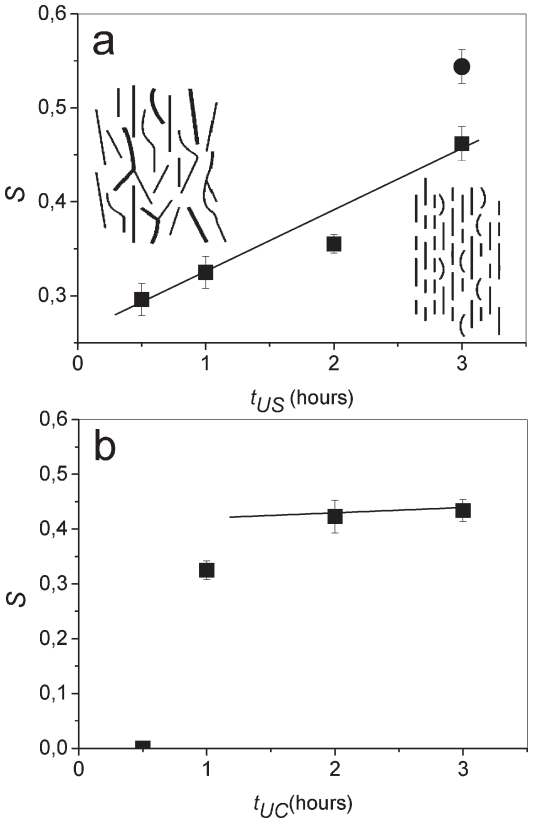

Figure 4. (a) Order parameter of nematic dried films made with CNT dispersions that have been sonicated during different times t_{US}. All of the used dispersions have undergone a single ultracentrifugation step of 1 h at 210 000 g. The black circle shows the order parameter of a sample that has undergone a supplementary ultracentrifugation step during 45 min. The left schematic shows the poor ordering in weakly sonicated nanotubes. Some branched nanotubes and wavy ones with kinks can act as disordering species. Improvement of alignment, as sketched in the right schematic, is brought by sonication induced shortening and nanotube sorting by ultracentrifugation. (b) Order parameter of nematic dried films made with CNT dispersions that have been ultracentrifuged during different times t_{UC}. All of the used dispersions were sonicated during 2 h.

long sonication times. In addition, ultracentrifugation being known to be efficient at sorting nanotubes by their length[48] can provide another approach for selecting shortened nanotubes and check the hypothesis that shortened nanotubes exhibit a greater order parameter. The value of *S* as a function of the ultracentrifugation time t_{UC} is shown in part b of Figure 4. Each sample has been sonicated during 2 h. For the first sample at t_{UC} = 30 min, no ordering could be detected via optical microscopy under crossed polarizers. Raman spectroscopy experiments confirmed a random orientation of the nanotubes after a short ultracentrifugation time ($S = 0$). As shown in Figure 2, samples after a short ultracentrifugation times still contain wavy or branched nanotubes. Those particles act as disordering agents and prevent the formation of a nematic phase. After a longer ultracentrifugation time, the nematic order appears and increases strongly until a constant regime is reached at about t_{UC} = 2 h. This result indicates that nematic ordering is mostly hindered by long CNTs that sediment at short times. In view of this, we prepared a sample by performing an additional 45 min long ultracentrifugation step right after sonication (t_{US} = 3 h) to remove the longest and wavy

dx.doi.org/10.1021/jp1102077 |J. Phys. Chem. C 2011, 115, 3272–3278

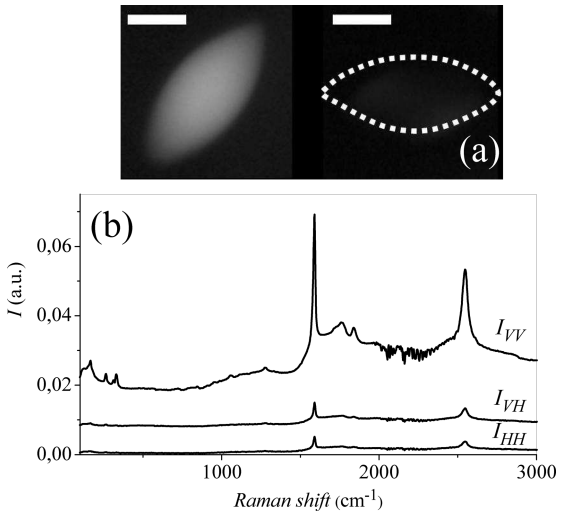

Figure 5. (a) Optical micrographs under polarizers crossed in vertical and horizontal directions of a nematic tactoid surrounded by the isotropic liquid phase. Scale bar 10 μm. (b) Raman scattered intensities of a nematic tactoid: I_{VV}, I_{VH}, and I_{HH}. The V axis corresponds to the long axis of the tactoid.

nanotubes. The sample was then treated as other samples previously described. The orentational order of this material is greatly improved compared to other samples. As shown in part a of Figure 4, S can increase up to 0.55 confirming thereby the negative influence of materials that quickly sediment. Such materials can contain tiny aggregates even after a long sonication time or tortuous and branched nanotubes that introduce an orientational disorder.

The isotropic-to-nematic phase transition can also be used to sort nanotubes by their capability of forming a liquid crystalline phase. Indeed in such polydisperse systems the nematic phase in equilibrium with an isotropic one is expected to be enriched with the straighter nanotubes that exhibit the greatest aspect ratio.[50] This offers an additional opportunity to select nanotubes for achieving more ordered nematics. Samples are prepared in the nematic−isotropic two phases region (with a weight fraction of nanotubes typically between 3 and 5 wt %) by diluting a nematic sample in an appropriate volume of aqueous bile salts solution (0.5 wt % in water). The diluted system is observed under optical microscopy. When the isotropic phase is in large excess, the nematic phase forms small spindlelike droplets as shown in part a of Figure 5. Their shape is reminiscent of nematic tactoids[52] found in the dispersions of highly anisometric colloidal particles such as metal oxides or fd viruses, considered as model system of rodlike particles.[37,38,41] Under crossed polarizers, the smallest ones can be uniformly extinct depending on their orientation relative to the polarizers. This shows the spontaneous and uniform alignment of the nanotubes with a total absence of heterogeneities that inherently exist in the bulk nematic phase. The nanotubes are uniformly oriented along the main axis of the spindles as shown by the maximal absorption of a polarized light when removing the analyzer. The elongated shape of the smallest tactoids and the uniform alignment of the nanotubes can be explained by considering the elastic energy cost of nematic distortions and the anisotropic and bare interfacial tensions of the isotropic−nematic interface.[53] The shape of the present tactoids is discussed in a recent article[52] and is out of the scope of the present study. Nevertheless, these droplets are ideal candidates for precisely measuring the order parameter of a nanotube liquid crystal in the absence of heterogeneities. Indeed tactoids can be of several micrometers in length and diameter. They are examined under the micro-Raman spectroscope with an incident beam diameter focused in a 10 μm diameter spot. Care was taken to analyze only droplets larger than the beam size. This procedure also ensures that the tactoids occupy the whole thickness of the cell. The latter is of 10 μm. In such conditions, the recorded signal comes only from the tactoid nematic phase. The scattered intensities I_{VV}, I_{VH}, and I_{HH} of an individual tactoid are shown in part b of Figure 5. The V axis corresponds to the long axis of the tactoid. Photoluminescence is clearly seen in the spectra and confirms the presence of individual nanotubes. The order parameter can be deduced from such measurements for tactoids obtained with dispersions achieved after different sonication times. The order parameter is found to be nearly the same with $S = 0.63$ for $t_{US} = 1$ h and $t_{UC} = 2$ h, and $S = 0.65$ for $t_{US} = 3$ h and $t_{UC} = 2$ h. This value of order parameter is greater than the one observed for bulk materials. It approaches the value theoretically expected for ideal hard rods. This observation is consistent with the absence of heterogeneities, and suggests also that the phase-separation process spontaneously selects the CNTs that promote nematic ordering, that is the nanotubes that do not introduce orientational disorder. The typical value of $S = 0.65$ does not increase with sonication time and is presumably the optimal value for the present nanotubes at the nematic−isotropic phase equilibrium.

CONCLUSIONS

This study shows that the liquid crystal properties of CNTs are extremely sensitive to their morphology and dispersion processing. Sonication and ultracentrifugation allowed sorting CNTs as a function of their length. Short nanotubes that have been exposed to strong and long sonication are found to form highly ordered liquid crystals. The isotropic−nematic phase-separation process was also found to be effective at selecting the best liquid crystal forming nanotubes. Such materials when confined into droplets at the isotropic−nematic transition can form nematic tactoids that exhibit a uniform orientation. These materials were used to measure the order parameter of a nanotube-based nematic in ideal conditions. The value of this order parameter was found to be much greater than that of bulk nanotube liquid crystals. Sorting nanotubes via phase-separation processes or dispersion processing are therefore efficient routes toward highly ordered CNT liquid crystals. Future challenges will consist of using these new materials to manifest the properties of ordered nanotubes in applications and devices.

AUTHOR INFORMATION

Corresponding Author

*E-mail: poulin@crpp-bordeaux.cnrs.fr.

REFERENCES

(1) Joselevich, E.; Dai, H. J.; Liu, J.; Hata, K.; Windle, A. H. Carbon nanotube synthesis and organization. In *Carbon Nanotubes*; Springer-Verlag: Berlin, 2008; Vol. 111, pp 101−164.

(2) Camponeschi, E.; Vance, R.; Al-Haik, M.; Garmestani, H.; Tannenbaum, R. Properties of carbon nanotube-polymer composites aligned in a magnetic field. *Carbon* **2007**, *45* (10), 2037–2046.

(3) Choi, E. S.; Brooks, J. S.; Eaton, D. L.; Al-Haik, M. S.; Hussaini, M. Y.; Garmestani, H.; Li, D.; Dahmen, K. Enhancement of thermal and

electrical properties of carbon nanotube polymer composites by magnetic field processing. *J. Appl. Phys.* **2003**, *94* (9), 6034–6039.

(4) Kordas, K.; Mustonen, T.; Toth, G.; Vahakangas, J.; Uusimaki, A.; Jantunen, H.; Gupta, A.; Rao, K. V.; Vajtai, R.; Ajayan, P. M. Magnetic-field induced efficient alignment of carbon nanotubes in aqueous solutions. *Chem. Mater.* **2007**, *19* (4), 787–791.

(5) Hone, J.; Llaguno, M. C.; Nemes, N. M.; Johnson, A. T.; Fischer, J. E.; Walters, D. A.; Casavant, M. J.; Schmidt, J.; Smalley, R. E. Electrical and thermal transport properties of magnetically aligned single wall carbon nanotube films. *Appl. Phys. Lett.* **2000**, *77* (5), 666–668.

(6) Behabtu, N.; Green, M. J.; Pasquali, M. Carbon nanotube-based neat fibers. *Nano Today* **2008**, *3* (5−6), 24–34.

(7) Vigolo, B.; Penicaud, A.; Coulon, C.; Sauder, C.; Pailler, R.; Journet, C.; Bernier, P.; Poulin, P. Macroscopic fibers and ribbons of oriented carbon nanotubes. *Science* **2000**, *290* (5495), 1331–1334.

(8) Ericson, L. M.; Fan, H.; Peng, H. Q.; Davis, V. A.; Zhou, W.; Sulpizio, J.; Wang, Y. H.; Booker, R.; Vavro, J.; Guthy, C.; Parra-Vasquez, A. N. G.; Kim, M. J.; Ramesh, S.; Saini, R. K.; Kittrell, C.; Lavin, G.; Schmidt, H.; Adams, W. W.; Billups, W. E.; Pasquali, M.; Hwang, W. F.; Hauge, R. H.; Fischer, J. E.; Smalley, R. E. Macroscopic, neat, single-walled carbon nanotube fibers. *Science* **2004**, *305* (5689), 1447–1450.

(9) Miaudet, P.; Badaire, S.; Maugey, M.; Derre, A.; Pichot, V.; Launois, P.; Poulin, P.; Zakri, C. Hot-drawing of single and multiwall carbon nanotube fibers for high toughness and alignment. *Nano Lett.* **2005**, *5* (11), 2212–2215.

(10) Li, Y. L.; Kinloch, I. A.; Windle, A. H. Direct spinning of carbon nanotube fibers from chemical vapor deposition synthesis. *Science* **2004**, *304* (5668), 276–278.

(11) Zhang, X. F.; Li, Q. W.; Holesinger, T. G.; Arendt, P. N.; Huang, J. Y.; Kirven, P. D.; Clapp, T. G.; DePaula, R. F.; Liao, X. Z.; Zhao, Y. H.; Zheng, L. X.; Peterson, D. E.; Zhu, Y. T., Ultrastrong, stiff, and lightweight carbon-nanotube fibers. *Adv. Mater.* **2007**, *19* (23), 4198-+.

(12) Scalia, G. Alignment of carbon nanotubes in thermotropic and lyotropic liquid crystals. *Chemphyschem* **2010**, *11* (2), 333–340.

(13) Lynch, M. D.; Patrick, D. L. Organizing carbon nanotubes with liquid crystals. *Nano Lett.* **2002**, *2* (11), 1197–1201.

(14) Shah, H. J.; Fontecchio, A. K.; Mattia, D.; Gogotsi, Y. Field controlled nematic-to-isotropic phase transition in liquid crystal-carbon nanotube composites. *J. Appl. Phys.* **2008**, *103* (6), 064314.

(15) Weiss, V.; Thiruvengadathan, R.; Regev, O. Preparation and characterization of a carbon nanotube-lyotropic liquid crystal composite. *Langmuir* **2006**, *22* (3), 854–856.

(16) van der Schoot, P.; Popa-Nita, V.; Kralj, S. Alignment of carbon nanotubes in nematic liquid crystals. *J. Phys. Chem. B* **2008**, *112* (15), 4512–4518.

(17) Lagerwall, J. P. F.; Scalia, G. Carbon nanotubes in liquid crystals. *J. Mater. Chem.* **2008**, *18* (25), 2890–2898.

(18) Lagerwall, J.; Scalia, G.; Haluska, M.; Dettlaff-Weglikowska, U.; Roth, S.; Giesselmann, F., Nanotube alignment using lyotropic liquid crystals. *Adv. Mater.* **2007**, *19* (3), 359-+.

(19) Dierking, I.; Scalia, G.; Morales, P. Liquid crystal-carbon nanotube dispersions. *J. Appl. Phys.* **2005**, *97* (4), 044309.

(20) Zhang, S. J.; Kumar, S. Carbon nanotubes as liquid crystals. *Small* **2008**, *4* (9), 1270–12831.

(21) Song, W. H.; Kinloch, I. A.; Windle, A. H. Nematic liquid crystallinity of multiwall carbon nanotubes. *Science* **2003**, *302* (5649), 1363–1363.

(22) Zakri, C.; Poulin, P. Phase behavior of nanotube suspensions: from attraction induced percolation to liquid crystalline phases. *J. Mater. Chem.* **2006**, *16* (42), 4095–4098.

(23) Badaire, S.; Zakri, C.; Maugey, M.; Derre, A.; Barisci, J. N.; Wallace, G.; Poulin, P., Liquid crystals of DNA-stabilized carbon nanotubes. *Adv. Mater.* **2005**, *17* (13), 1673-+.

(24) Islam, M. F.; Alsayed, A. M.; Dogic, Z.; Zhang, J.; Lubensky, T. C.; Yodh, A. G. Nematic nanotube gels. *Phys. Rev. Lett.* **2004**, *92* (8), 088303−1–088303−4.

(25) Moulton, S. E.; Maugey, M.; Poulin, P.; Wallace, G. G. Liquid crystal behavior of single-walled carbon nanotubes dispersed in biological hyaluronic acid solutions. *J. Am. Chem. Soc.* **2007**, *129* (30), 9452–9457.

(26) Rai, P. K.; Pinnick, R. A.; Parra-Vasquez, A. N. G.; Davis, V. A.; Schmidt, H. K.; Hauge, R. H.; Smalley, R. E.; Pasquali, M. Isotropic-nematic phase transition of single-walled carbon nanotubes in strong acids. *J. Am. Chem. Soc.* **2006**, *128* (2), 591–595.

(27) Lu, L. H.; Chen, W. Large-scale aligned carbon nanotubes from their purified, highly concentrated suspension. *ACS Nano* **2010**, *4* (2), 1042–1048.

(28) Zamora-Ledezma, C.; Blanc, C.; Maugey, M.; Zakri, C.; Poulin, P.; Anglaret, E. Anisotropic thin films of single-wall carbon nanotubes from aligned lyotropic nematic suspensions. *Nano Lett.* **2008**, *8* (12), 4103–4107.

(29) Song, W. H.; Windle, A. H. Isotropic-nematic phase transition of dispersions of multiwall carbon nanotubes. *Macromolecules* **2005**, *38* (14), 6181–6188.

(30) Zhang, S. J.; Kinloch, I. A.; Windle, A. H. Mesogenicity drives fractionation in lyotropic aqueous suspensions of multiwall carbon nanotubes. *Nano Lett.* **2006**, *6* (3), 568–572.

(31) Song, W. H.; Windle, A. H. Size-dependence and elasticity of liquid-crystalline multiwalled carbon nanotubes. *Adv. Mater.* **2008**, *20* (16), 3149–3154.

(32) Davis, V. A.; Parra-Vasquez, A. N. G.; Green, M. J.; Rai, P. K.; Behabtu, N.; Prieto, V.; Booker, R. D.; Schmidt, J.; Kesselman, E.; Zhou, W.; Fan, H.; Adams, W. W.; Hauge, R. H.; Fischer, J. E.; Cohen, Y.; Talmon, Y.; Smalley, R. E.; Pasquali, M. True solutions of single-walled carbon nanotubes for assembly into macroscopic materials. *Nature Nanotechnol.* **2009**, *4* (12), 830–834.

(33) Zhang, S. J.; Li, Q. W.; Kinloch, I. A.; Windle, A. H. Ordering in a droplet of an aqueous suspension of single-wall carbon nanotubes on a solid substrate. *Langmuir* **2010**, *26* (3), 2107–2112.

(34) Vroege, G. J.; Lekkerkerker, H. N. W. Phase-transitions in lyotropic colloidal and polymer liquid-crystals. *Rep. Prog. Phys.* **1992**, *55* (8), 1241–1309.

(35) Davidson, P.; Gabriel, J. C. P. Mineral liquid crystals. *Curr. Opin. Colloid Interface Sci.* **2005**, *9* (6), 377–383.

(36) Lima, M. M. D.; Borsali, R. Rodlike cellulose microcrystals: Structure, properties, and applications. *Macromol. Rapid Commun.* **2004**, *25* (7), 771–787.

(37) Dogic, Z.; Fraden, S. Ordered phases of filamentous viruses. *Curr. Opin. Colloid Interface Sci.* **2006**, *11* (1), 47–55.

(38) Grelet, E. Hexagonal order in crystalline and columnar phases of hard rods. *Phys. Rev. Lett.* **2008**, *100* (16), 168301–1−168301−4.

(39) Onsager, L. The effects of shape on the interaction of colloidal particles. *Ann. N.Y. Acad. Sci.* **1949**, *51* (4), 627–659.

(40) Grelet, E.; Fraden, S. What is the origin of chirality in the cholesteric phase of virus suspensions?. *Phys. Rev. Lett.* **2003**, *90* (19), 198302.

(41) Zhang, Z. K.; Krishna, N.; Lettinga, M. P.; Vermant, J.; Grelet, E. Reversible gelation of rod-like viruses grafted with thermoresponsive polymers. *Langmuir* **2009**, *25* (4), 2437–2442.

(42) Zamora-Ledezma, C.; Blanc, C.; Anglaret, E. Orientational order of single-wall carbon nanotubes in stretch-aligned photoluminescent composite films. *Phys. Rev. B* **2009**, *80* (11), 113407.

(43) Liu, C.; Muthukumar, M. Annihilation kinetics of liquid crystal defects. *J. Chem. Phys.* **1997**, *106* (18), 7822–7828.

(44) Chuang, I.; Yurke, B.; Pargellis, A. N.; Turok, N. Coarsening dynamics in uniaxial nematic liquid-crystals. *Phys. Rev. E* **1993**, *47* (5), 3343–3356.

(45) Badaire, S.; Poulin, P.; Maugey, M.; Zakri, C. In situ measurements of nanotube dimensions in suspensions by depolarized dynamic light scattering. *Langmuir* **2004**, *20* (24), 10367–10370.

(46) Lucas, A.; Zakri, C.; Maugey, M.; Pasquali, M.; van der Schoot, P.; Poulin, P. Kinetics of nanotube and microfiber scission under sonication. *J. Phys. Chem. C* **2009**, *113* (48), 20599–20605.

(47) Wenseleers, W.; Vlasov, I. I.; Goovaerts, E.; Obraztsova, E. D.; Lobach, A. S.; Bouwen, A. Efficient isolation and solubilization of pristine single-walled nanotubes in bile salt micelles. *Adv. Funct. Mater.* **2004**, *14* (11), 1105–1112.

(48) Fagan, J. A.; Becker, M. L.; Chun, J.; Hobbie, E. K., Length fractionation of carbon nanotubes using centrifugation. *Adv. Mater.* **2008**, *20* (9), 1609-+.

(49) Dresselhaus, M. S.; Dresselhaus, G.; Saito, R.; Jorio, A. Raman spectroscopy of carbon nanotubes. *Physics Reports-Review Section of Physics Letters* **2005**, *409* (2), 47–99.

(50) Haggenmueller, R.; Rahatekar, S. S.; Fagan, J. A.; Chun, J. H.; Becker, M. L.; Naik, R. R.; Krauss, T.; Carlson, L.; Kadla, J. F.; Trulove, P. C.; Fox, D. F.; DeLong, H. C.; Fang, Z. C.; Kelley, S. O.; Gilman, J. W. Comparison of the quality of aqueous dispersions of single wall carbon nanotubes using surfactants and biomolecules. *Langmuir* **2008**, *24* (9), 5070–5078.

(51) Lekkerkerker, H. N. W.; Coulon, P.; Vanderhaegen, R.; Deblieck, R. On the isotropic-liquid crystal phase-separation in a solution of rodlike particles of different lengths. *J. Chem. Phys.* **1984**, *80* (7), 3427–3433.

(52) Puech, N.; Grelet, E.; Poulin, P.; Blanc, C.; van der Schoot, P. Nematic droplets in aqueous dispersions of carbon nanotubes. *Phys. Rev. E* **2010**, *82* (2), 020702.

(53) Prinsen, P.; van der Schoot, P. Shape and director-field transformation of tactoids. *Phys. Rev. E* **2003**, *68* (2), 021701.